

PAPER • OPEN ACCESS

## Structural and Electrochemical Properties of Layered-Layered-Spinel Composite Cathode Materials $\text{Li}_x\text{Mn}_{4/6}\text{Ni}_{1/6}\text{Co}_{1/6}\text{O}_{(1.75+0.5x)}$ ( $1.1 \leq x \leq 1.3$ ) for Lithium-Ion Batteries

To cite this article: Zhu Zhenye 2019 *IOP Conf. Ser.: Mater. Sci. Eng.* **544** 012044

View the [article online](#) for updates and enhancements.



**IOP | ebooks™**

Bringing you innovative digital publishing with leading voices to create your essential collection of books in STEM research.

Start exploring the collection - download the first chapter of every title for free.

# Structural and Electrochemical Properties of Layered-Layered-Spinel Composite Cathode Materials $\text{Li}_x\text{Mn}_{4/6}\text{Ni}_{1/6}\text{Co}_{1/6}\text{O}_{(1.75+0.5x)}$ ( $1.1 \leq x \leq 1.3$ ) for Lithium-Ion Batteries

Zhu Zhenye

School of Materials Science and Engineering, Habin Institute of Technology (Shenzhen) 518055, PR China

Corresponding author: [zhuzy@hit.edu.cn](mailto:zhuzy@hit.edu.cn)

**Abstract.** The cathode materials  $\text{Li}_x\text{Mn}_{4/6}\text{Ni}_{1/6}\text{Co}_{1/6}\text{O}_{(1.75+0.5x)}$  ( $x=1.1, 1.2, 1.3$ ) with different content of lithium have been synthesized by two step temperature co-precipitation in this paper. X-ray diffraction patterns confirm that there are spinel structure and layer structure in prepared composite. SEM images show that the same diameters of the assembled microspheres are at about 4  $\mu\text{m}$  in  $\text{Li}_x\text{Mn}_{4/6}\text{Ni}_{1/6}\text{Co}_{1/6}\text{O}_{(1.75+0.5x)}$  composite. The measurement of electrochemical properties indicates that, with content of lithium varying from 1.1 to 1.3, content of spinel component declines, which induce to the increase of discharge capacity and decrease of capacity retention.  $\text{Li}_{1.1}\text{Mn}_{4/6}\text{Ni}_{1/6}\text{Co}_{1/6}\text{O}_{2.30}$  composite delivers best rate capability, because there is more spinel component in  $\text{Li}_{1.1}\text{Mn}_{4/6}\text{Ni}_{1/6}\text{Co}_{1/6}\text{O}_{2.30}$ .

## 1. Introduction

The exploration and development of cathode materials in lithium-ion batteries with high capacity, good cycling stability, and low cost are of great importance, owing to the widespread applications of lithium-ion batteries in people's daily life [1-3]. However, for market requirements their available energy density is still a defect. As a result, much effort on improving energy efficiency and reducing environmental pollution should be done in the future. The commercially available  $\text{LiCoO}_2$  cathode suffers from lack of further development and application because of its high cost, low capacity and toxicity [4]. Doped material  $\text{LiNi}_{1/3}\text{Co}_{1/3}\text{Mn}_{1/3}\text{O}_2$  was initially synthesized in 2001 by Ohzuku and Makimura, which was considered as a promising cathode material for Li-ion batteries (LIBs) because of its milder thermal stability, lower cost, and excellent cycling performance [5-6]. Layered  $\text{LiMnO}_2$  also showed structural transformation to spinel during electrochemical cycling [7,8]. A layered  $\text{LiNi}_{0.5}\text{Mn}_{0.5}\text{O}_2$  material prepared by coprecipitation method showed promising capacity of around 150  $\text{mA}\cdot\text{h/g}$  in the voltage range of 2.5–4.3V [9]. Kang et al. [10] have reported increased discharge capacity and electrical conductivity by doping Al, Ti, and Co in  $\text{LiNi}_{0.5}\text{Mn}_{0.5}\text{O}_2$ . Among those materials, Co doping increased electrical conductivity most successfully.

Cathode materials with different stoichiometry containing lithium manganese oxide ( $\text{Li}_2\text{MnO}_3$ ) and lithium metal oxide [ $\text{LiMeO}_2$  (Me = Co, Ni, Mn, etc.)] have been studied in the recent years and are considered as potential candidates to replace the commercial lithium cobalt (III) oxide ( $\text{LiCoO}_2$ ). These mainly include  $\text{Li}_{1.2}\text{Ni}_{0.2}\text{Mn}_{0.6}\text{O}_2$  [ $0.5\text{Li}_2\text{MnO}_3 \cdot 0.5\text{LiNi}_{0.5}\text{Mn}_{0.5}\text{O}_2$ ] and  $\text{Li}_{1.2}\text{Ni}_{0.13}\text{Co}_{0.13}\text{Mn}_{0.54}\text{O}_2$  [ $0.5\text{Li}_2\text{MnO}_3 \cdot 0.5\text{LiNi}_{0.33}\text{Mn}_{0.33}\text{Co}_{0.33}\text{O}_2$ ] [11,12]. The use of the cobalt reduces the electrode polarization.  $\text{Li}_2\text{MnO}_3$  is known to be electrochemically inactive because of the presence of Mn in its +4 oxidation



state. However, when charged above 4.5 V, this material can apparently become electrochemically active due to the extraction of Li and O, which in turn leads to the formation of the manganese dioxide ( $\text{MnO}_2$ ) host structure in the compound, which can then reversibly intercalate lithium ions [13-15]. In recent years, the lithium-ion layered solid solutions in a chemical formula of  $y\text{Li}_2\text{MnO}_3 \cdot (1-y)\text{LiMO}_2$  ( $0 < y < 1$ ;  $\text{M} = \text{Ni, Co, Mn, Fe, Cr, Ni}_{1/2}\text{Mn}_{1/2}, \text{Ni}_{1/3}\text{Co}_{1/3}\text{Mn}_{1/3}$ , etc.) have attracted more and more attention from specialists and have been recognized as one of the most promising candidates for the next generation of lithium-ion batteries [16-19].

## 2. Experimental

### 2.1 Synthesis: two-step co-precipitation method

Layer-layer-spinel structure  $\text{Li}_{1.2}\text{Mn}_{4/6}\text{Ni}_{1/6}\text{Co}_{1/6}\text{O}_{2.35-x}\text{F}_x$  ( $x=0, 0.05, 0.10, 0.15$ ) cathode material was synthesized by two-step co-precipitation method. Figure 1 and Figure 2 show the preparation procedure of the precursor  $[\text{Mn}_{4/6}\text{Ni}_{1/6}\text{Co}_{1/6}]\text{CO}_3$  and the cathode material  $\text{Li}_x\text{Mn}_{4/6}\text{Ni}_{1/6}\text{Co}_{1/6}\text{O}_{(1.75+0.5x)}$  ( $x=1.1, 1.2, 1.3$ ).

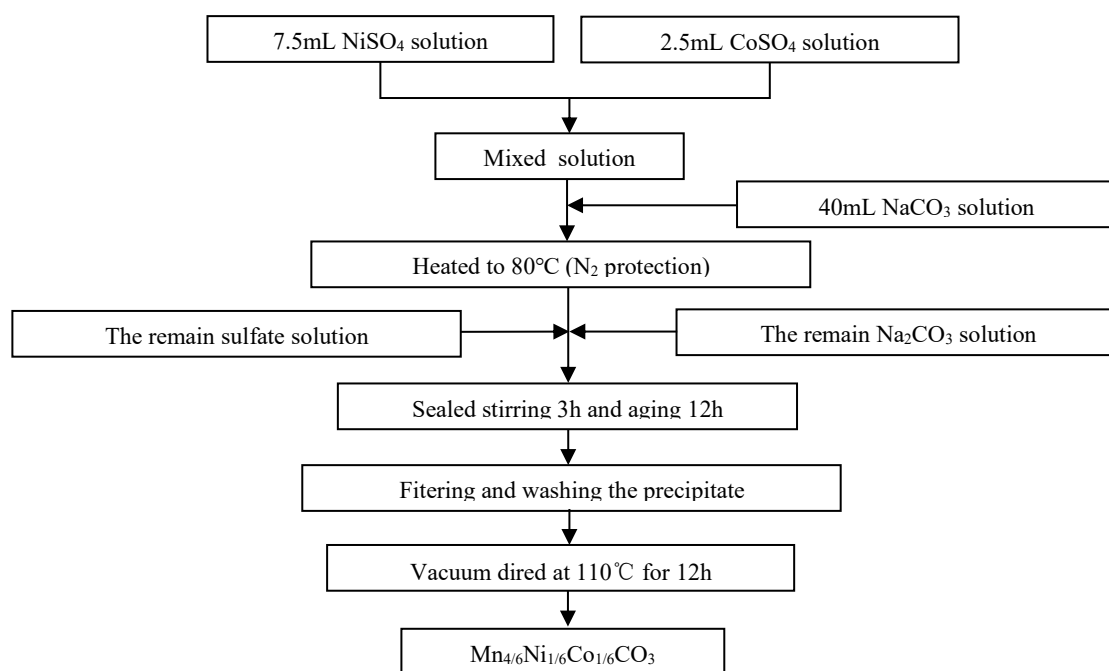


**Figure 1.** Schematic diagram of the synthesis of precursor  $[\text{Mn}_{4/6}\text{Ni}_{1/6}\text{Co}_{1/6}]\text{CO}_3$

Firstly, the aqueous solution was prepared by dissolving the salts of  $\text{NiSO}_4 \cdot 7\text{H}_2\text{O}$  (Shanghai Aladdin, 99.9%) ,  $\text{CoSO}_4 \cdot 7\text{H}_2\text{O}$  (Shanghai Aladdin, 99.999%) and  $\text{MnSO}_4 \cdot \text{H}_2\text{O}$  (Shanghai Aladdin, 99%) in distilled water with a concentration of  $1\text{molL}^{-1}$ , and dissolving the  $\text{NaCO}_3$  in distilled water with a concentration of  $0.3\text{molL}^{-1}$ . Secondly,  $\text{NiSO}_4 \cdot 7\text{H}_2\text{O}$  and  $\text{CoSO}_4 \cdot 7\text{H}_2\text{O}$  with a mount of 7.5ml an 2.5ml were pumped into the reaction tank together and 40mL  $\text{NaCO}_3$  aqueous solution was added dropwise to reaction tank, and the mixed solution was stirred and maintained at  $40^\circ\text{C}$ . Let the reaction temperature raise to  $80^\circ\text{C}$  after completion of the dropwise-addition, and then the mixed solution (2.5mL  $\text{NiSO}_4 \cdot 7\text{H}_2\text{O}$ , 7.5mL  $\text{CoSO}_4 \cdot 7\text{H}_2\text{O}$  and 40mL  $\text{MnSO}_4 \cdot \text{H}_2\text{O}$ ) were added dropwise into the continuous stirred (900r/min) solution in the reaction tank, while the required  $\text{NaCO}_3$  was also dropped into the reactor drop by drop. After the completion of the precipitation reaction, the mixed solution was stirred for 3h at the constant temperature and then aged over night. the precursor was washed for several times with the distilled water and dried in vacuum at  $110^\circ\text{C}$  for 12h. Then, 5%

excess  $\text{LiCO}_3$  were mixed thoroughly with the obtained  $[\text{Mn}_{4/6}\text{Ni}_{1/6}\text{Co}_{1/6}]\text{CO}_3$ , and first fired at  $500^\circ\text{C}$  for 5h and then  $850^\circ\text{C}$  for 15h in air with a heating rate of  $5^\circ\text{C}/\text{min}$ .

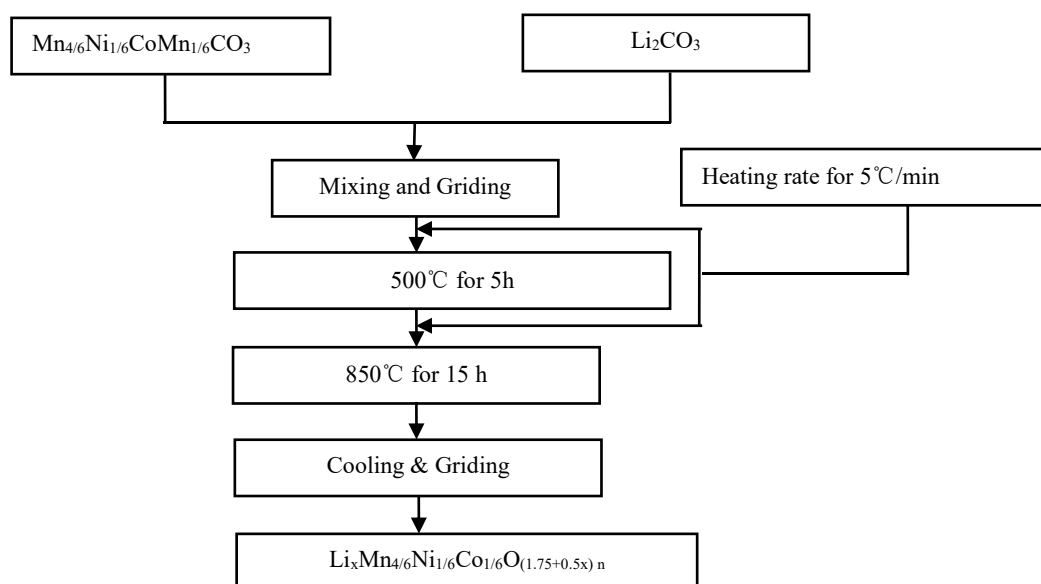


**Figure 2.** Schematic diagram of the synthesis of cathode material  $\text{Li}_x\text{Mn}_{4/6}\text{Ni}_{1/6}\text{Co}_{1/6}\text{O}_{(1.75+0.5x)n}$ .

## 2.2 Structure and morphology

A powder X-ray diffractometer (XRD, Rigaku RINT2000 with  $\text{Cu-K}\alpha$  radiation) in a range of  $2\theta=10^\circ\text{--}80^\circ$  with a scan rate of  $6^\circ\text{min}^{-1}$  was employed to analyze the structure and phase composition of synthesized samples. The scanning electron microscopy (SEM, Hitachi S4700) images were taken to get the morphology and size of the samples.

## 2.3 Electrochemical measurements

The electrochemical properties of the synthesized samples were examined using a coin cells (CR2032). The coin type half-cell contains cathode and Li metal anode, which were separated by a porous polypropylene film (Celgard 2400) and electrolyte consisting 1M  $\text{LiPF}_6$  (EC:DMC=1: 1 in volume). The positive electrode was prepared by spreading mixture of prepared powders (80wt.%), carbon conducting additive (Super-P Li 10wt.%) and polyvinylidene flouride (PVDF 10wt.%) dissolved in N-methyl-2-pyrrolidone (NMP) onto a smooth aluminum foil. The positive electrode was allowed to dry at  $75^\circ\text{C}$  for 3h in the air and then at  $120^\circ\text{C}$  for 10h in a vacuum oven. The resulting electrode film was then punched into circular discs. The charge-discharge tests were set in the voltage range of 2.0-4.8V ( $1\text{C}=250\text{mAhg}^{-1}$ ). The electrochemical measurements were carried out by using the Solartron Electrochemical workstation.

## 3. Results and discussion

### 3.1 Structure of $[\text{Mn}_{4/6}\text{Ni}_{1/6}\text{Co}_{1/6}]\text{CO}_3$ precursor

Figure 3 shows the XRD diffraction peak of the precursor, and there is no extra hetero peak, which is consistent with characteristic diffraction peaks of standard card (PDF#44-1472). Figure 3 shows that our cathode materials synthesized precursor  $[\text{Mn}_{4/6}\text{Ni}_{1/6}\text{Co}_{1/6}]\text{CO}_3$  has  $\text{MnCO}_3$  type phase, which is trigonal calcite crystal phase.

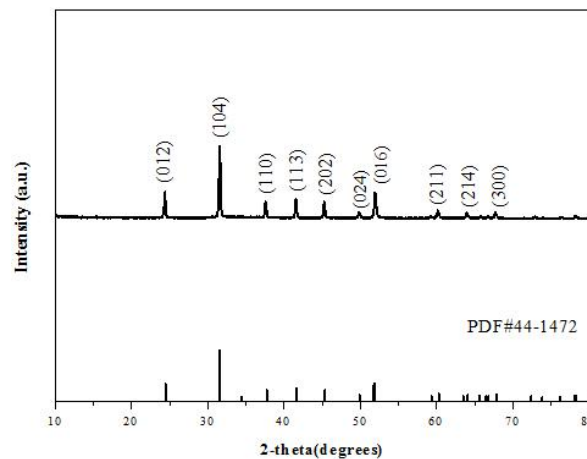


**Figure 3.** XRD patterns of  $\text{Mn}_{4/6}\text{Ni}_{1/6}\text{CO}_3$  precursor materials.

### 3.2 Structure and morphology of $\text{Li}_x\text{Mn}_{4/6}\text{Ni}_{1/6}\text{Co}_{1/6}\text{O}_{(1.75+0.5x)}$ ( $x=1.1, 1.2, 1.3$ ) composites

XRD patterns of synthesized  $\text{Li}_x\text{Mn}_{4/6}\text{Ni}_{1/6}\text{Co}_{1/6}\text{O}_{(1.75+0.5x)}$  ( $x=1.1, 1.2, 1.3$ ) composites are presented in Figure 4. In Figure 4, the diffraction peaks are very clear and sharp, and synthesized materials have relatively good crystallinity and relatively complete crystal form. Compared with the standard cards, the diffraction peaks are consistent with the standard peak  $\text{LiNi}_{0.5}\text{Mn}_{1.5}\text{O}_4$  cubic spinel materials (PDF # No.80-2162) with Fd-3m space group, which indicate that the synthesized materials contain spinel material  $\text{LiNi}_{0.5}\text{Mn}_{1.5}\text{O}_4$ . In addition, several diffraction peaks are inconsistent with standard cubic spinel peak of  $\text{LiNi}_{0.5}\text{Mn}_{1.5}\text{O}_4$  materials (PDF # No.80-2162), and other phase exist in synthesized materials. The diffraction peaks at  $20^\circ\sim 25^\circ$  and  $63^\circ\sim 67^\circ$  refer to  $\text{Li}_2\text{MnO}_3$  phase (PDF # No.98-016-6861) and layered structure  $\text{LiMn}_{1/3}\text{Ni}_{1/3}\text{Co}_{1/3}\text{O}_2$  phase, respectively.

Figure 5 shows SEM images of synthesized  $\text{Li}_x\text{Mn}_{4/6}\text{Ni}_{1/6}\text{Co}_{1/6}\text{O}_{(1.75+0.5x)}$  ( $x=1.1, 1.2, 1.3$ ) composites. The diameters of the assembled microspheres of  $\text{Li}_x\text{Mn}_{4/6}\text{Ni}_{1/6}\text{Co}_{1/6}\text{O}_{(1.75+0.5x)}$  are almost the same at about  $4\ \mu\text{m}$ , and the average particle size of primary particles is 200 nm. Therefore, the content of lithium in the composites does not affect the morphology.

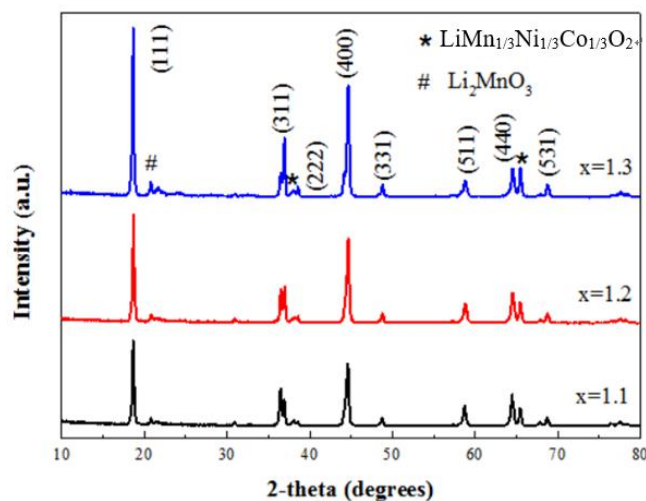


**Figure 4.** XRD patterns of  $\text{Li}_x\text{Mn}_{4/6}\text{Ni}_{1/6}\text{Co}_{1/6}\text{O}_{(1.75+0.5x)}$  ( $x=1.1, 1.2, 1.3$ ) materials.

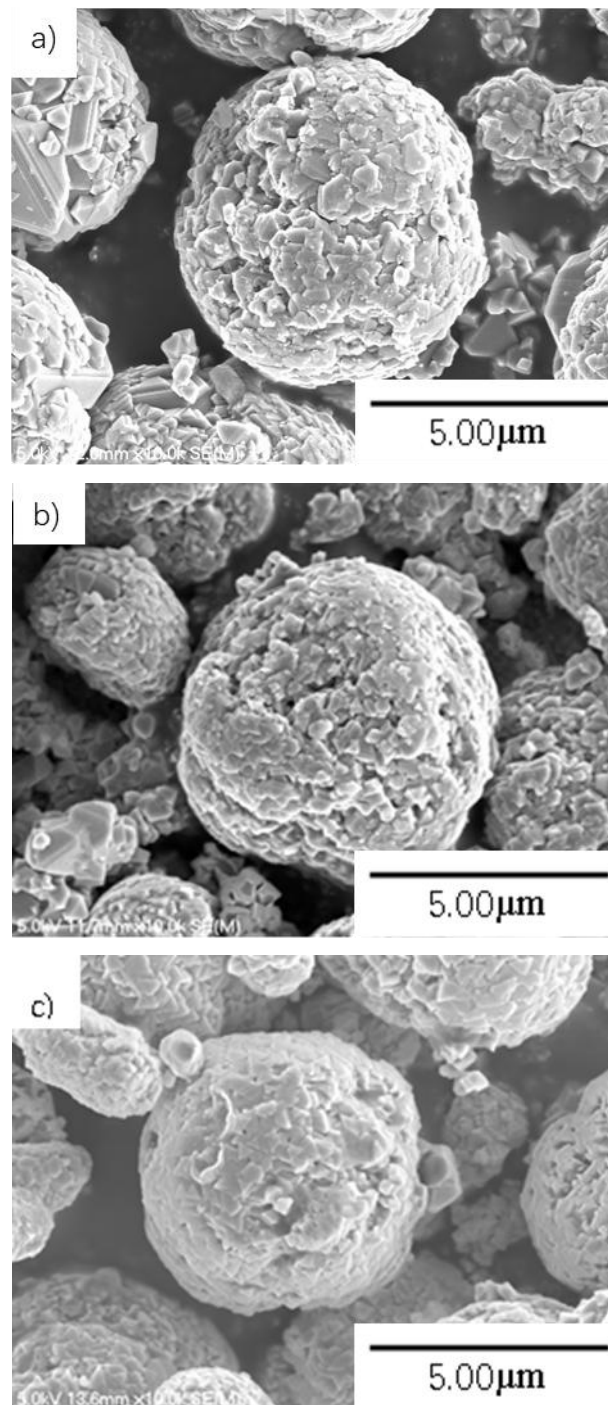


**Figure 5.** SEM images of  $\text{Li}_x\text{Mn}_{4/6}\text{Ni}_{1/6}\text{Co}_{1/6}\text{O}_{(1.75+0.5x)}$  ( $x=1.1, 1.2, 1.3$ )

a) $x=1.1$ , b) $x=1.2$ , c) $x=1.3$ .

### 3.3 Electrochemical performance

Figure 6 indicates that the discharge capacity of synthesized  $\text{Li}_x\text{Mn}_{4/6}\text{Ni}_{1/6}\text{Co}_{1/6}\text{O}_{(1.75+0.5x)}$  ( $x=1.1, 1.2, 1.3$ ) composites for 50 cycles at the current density of  $0.5\text{C}$  ( $125\text{mAhg}^{-1}$ ) in a voltage range of  $2.0\text{--}4.8\text{V}$ . As shown in Figure 6 a), with the content of lithium varying from  $1.1$  to  $1.3$ , discharge capacity gradually increases, Figure 6 b) shows the initial discharge capacity and cycle capacity retention rate of 50 times in  $\text{Li}_x\text{Mn}_{4/6}\text{Ni}_{1/6}\text{Co}_{1/6}\text{O}_{(1.75+0.5x)}$  ( $x=1.1, 1.2, 1.3$ ) composites. In Figure 6 b), the initial discharge capacity rises and the capacity retention decreases as the lithium content is increased. Spinel

structures in the  $\text{Li}_x\text{Mn}_{4/6}\text{Ni}_{1/6}\text{Co}_{1/6}\text{O}_{(1.75+0.5x)}$  composite become less and less as the content of lithium is creased.  $\text{Li}_{1.3}\text{Mn}_{4/6}\text{Ni}_{1/6}\text{Co}_{1/6}\text{O}_{2.4}$  deliver largest initial discharge capacity and smallest capacity retention. Since the spinel structure is stable and shows small discharge capacity, reduction of spinel structure will certainly affect the capacity retention rate of composite.

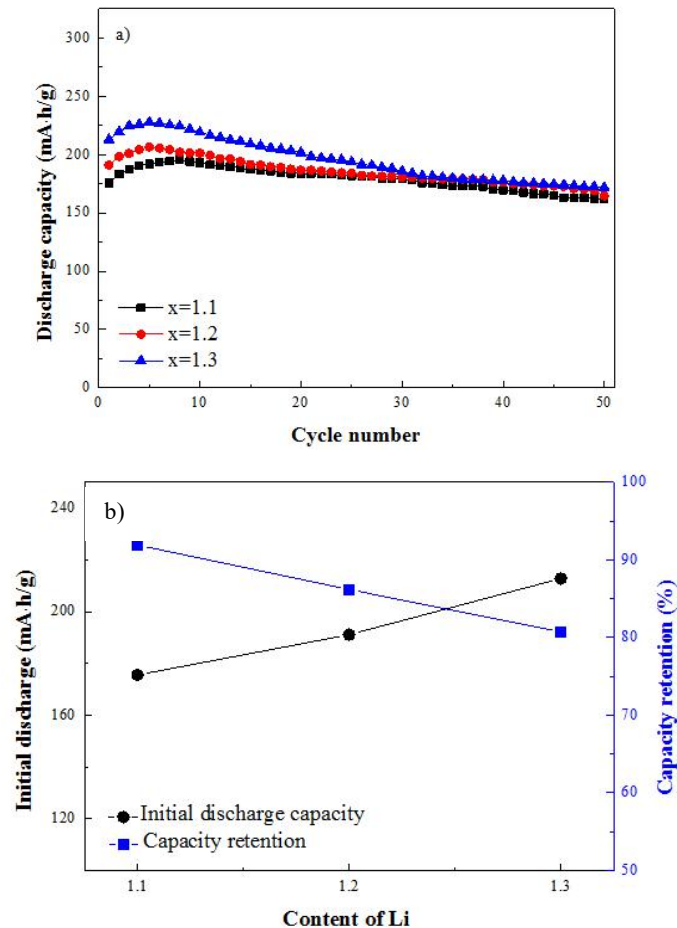


**Figure 6.** a) Cycle performance of  $\text{Li}_x\text{Mn}_{4/6}\text{Ni}_{1/6}\text{Co}_{1/6}\text{O}_{(1.75+0.5x)}$  ( $x=1.1, 1.2, 1.3$ ) at a discharge rate of 0.5C ( $1C=250\text{mA}\cdot\text{h}\cdot\text{g}^{-1}$ ), and b) the corresponding initial discharge capacity and capacity retention values.

Figure 7 shows the rate capability of the  $\text{Li}_x\text{Mn}_{4/6}\text{Ni}_{1/6}\text{Co}_{1/6}\text{O}_{(1.75+0.5x)}$  ( $x=1.1, 1.2, 1.3$ ) between 2.0V and 4.8V at charge-discharge rates from 0.1C to 5C ( $1C=250\text{mA}\cdot\text{h}\cdot\text{g}^{-1}$ ). In Figure 7, With the applied current density increasing, all discharge capacity of all composites decline gradually, to some degree, which can be ascribed to the increasing polarization of the electrodes at high current densities. All discharge capacity of  $\text{Li}_x\text{Mn}_{4/6}\text{Ni}_{1/6}\text{Co}_{1/6}\text{O}_{(1.75+0.5x)}$  ( $x=1.1, 1.2, 1.3$ ) at different current density are listed in Table 1. It is indicated that initial discharge capacity of  $\text{Li}_{1.3}\text{Mn}_{4/6}\text{Ni}_{1/6}\text{Co}_{1/6}\text{O}_{2.40}$  material is ( $259.6\text{mA}\cdot\text{h}\cdot\text{g}^{-1}$ ) was significantly better than that of the other two materials ( $241\text{mA}\cdot\text{h}\cdot\text{g}^{-1}$  and  $242\text{mA}\cdot\text{h}\cdot\text{g}^{-1}$ ). However, with charge-discharge current density increasing from 0.1C to 5C, the discharge capacity of  $\text{Li}_{1.3}\text{Mn}_{4/6}\text{Ni}_{1/6}\text{Co}_{1/6}\text{O}_{2.40}$  composite decrease greatly, achieving  $53.4\text{mA}\cdot\text{h}\cdot\text{g}^{-1}$  at 5C. When the charge-discharge current density is 5C,  $\text{Li}_{1.1}\text{Mn}_{4/6}\text{Ni}_{1/6}\text{Co}_{1/6}\text{O}_{2.30}$  has a maximum discharge capacity ( $78.6\text{mA}\cdot\text{h}\cdot\text{g}^{-1}$ ).  $\text{Li}_{1.1}\text{Mn}_{4/6}\text{Ni}_{1/6}\text{Co}_{1/6}\text{O}_{2.30}$  composite shows the best rate performance, because  $\text{Li}_{1.1}\text{Mn}_{4/6}\text{Ni}_{1/6}\text{Co}_{1/6}\text{O}_{2.30}$  composite contains more spinel component, which is beneficial to structural stability during charge-discharge process.

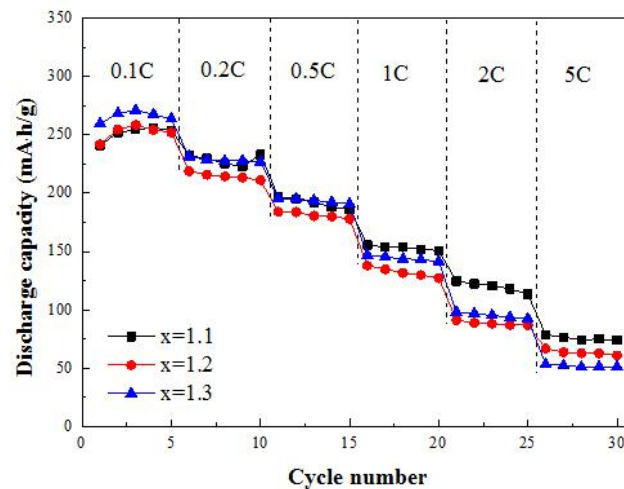


**Figure 7.** Rate capacity of  $\text{Li}_x\text{Mn}_{4/6}\text{Ni}_{1/6}\text{Co}_{1/6}\text{O}_{(1.75+0.5x)}$  ( $x=1.1, 1.2, 1.3$ ) in the voltage range of 2.0-4.8V.

**Table 1.** First discharge specific capacity at different rates

$\text{Li}_x\text{Mn}_{4/6}\text{Ni}_{1/6}\text{Co}_{1/6}\text{O}_{(1.75+0.5x)}$	First discharge specific capacity at different rates ( $\text{mA}\cdot\text{h/g}$ )					
	0.1C	0.2C	0.5C	1C	2C	5C
$\text{Li}_{1.1}\text{Mn}_{4/6}\text{Ni}_{1/6}\text{Co}_{1/6}\text{O}_{2.30}$	241	232.2	196.7	155.7	124.6	78.6
$\text{Li}_{1.2}\text{Mn}_{4/6}\text{Ni}_{1/6}\text{Co}_{1/6}\text{O}_{2.35}$	242	218.8	174.1	137.9	91.1	66.8
$\text{Li}_{1.3}\text{Mn}_{4/6}\text{Ni}_{1/6}\text{Co}_{1/6}\text{O}_{2.40}$	259.6	231.3	195.2	146.8	98	53.4

#### 4. Conclusion

The Layered-Layered-Spinel cathode materials  $\text{Li}_x\text{Mn}_{4/6}\text{Ni}_{1/6}\text{Co}_{1/6}\text{O}_{(1.75+0.5x)}$  ( $x=1.1, 1.2, 1.3$ ) with different lithium content have been synthesized by two-step co-precipitation method in this paper. Spinel phase and layer phase coexist in the  $\text{Li}_x\text{Mn}_{4/6}\text{Ni}_{1/6}\text{Co}_{1/6}\text{O}_{(1.75+0.5x)}$  ( $x=1.1, 1.2, 1.3$ ) composites. With the content of lithium increasing from 1.1 to 1.3, the initial discharge capacity of composite gradually increases and the retention of capacity declines, due to decrease of the spinel component.  $\text{Li}_{1.1}\text{Mn}_{4/6}\text{Ni}_{1/6}\text{Co}_{1/6}\text{O}_{2.30}$  composite deliver best rate capability, because there is more spinel component in  $\text{Li}_{1.1}\text{Mn}_{4/6}\text{Ni}_{1/6}\text{Co}_{1/6}\text{O}_{2.30}$ .

#### Acknowledgements

This work is supported by Shenzhen Basic Research Free Exploration Project (Nos.JCYJ20180306171650007).

#### References

- [1] Tarascon J M and Armand M B 2001 Issues and challenges facing rechargeable lithium batteries *Nature* **414**(6861) pp 359-367.



- [2] Whittingham M S 2004 Lithium batteries and cathode materials *Chemical Reviews* **35**(50) pp 4271-4302.
- [3] Arumugam D and Kalaigan G P 2010 Synthesis and electrochemical characterizations of nano- $\text{La}_2\text{O}_3$ -coated nanostructure  $\text{LiMn}_2\text{O}_4$  cathode materials for rechargeable lithium batteries *Materials Research Bulletin* **45**(12) pp 1825-1831.
- [4] Goodenough J B and Kim Y 2010 Challenges for rechargeable Li batteries *Chemistry of Materials* **22**(3) pp 587-603.
- [5] Yabuuchi N and Ohzuku T 2003 Novel lithium insertion material of  $\text{LiCo}_{1/3}\text{Ni}_{1/3}\text{Mn}_{1/3}\text{O}_2$  for advanced lithium-ion batteries *Journal of Power Sources* **119**(6) pp 171-174.
- [6] Lee M H, Kang Y, Myung S T and Sun Y K 2005 Synthetic optimization of  $\text{Li}[\text{Ni}_{1/3}\text{Co}_{1/3}\text{Mn}_{1/3}]\text{O}_2$  via co-precipitation *Electrochimica Acta* **50**(4) pp 939-948.
- [7] Ammundsen B and Paulsen J 2001 Novel lithium-ion cathode materials based on layered manganese oxides *Advanced Materials* **13**(12) pp 943-956.
- [8] Soo P P, Huang B, Jang Y I, et al 1999 Rubbery Block Copolymer Electrolytes for Solid-State Rechargeable Lithium Batteries *Journal of the Electrochemical Society* **146**(1) pp 32-37.
- [9] Yabuuchi N and Ohzuku T 2003 Novel lithium insertion material of  $\text{LiCo}_{1/3}\text{Ni}_{1/3}\text{Mn}_{1/3}\text{O}_2$ , for advanced lithium-ion batteries *Journal of Power Sources* **119**(6) pp 171-174.
- [10] S H Kang, J Kim, M E Stoll, D Abraham, Y K Sun, K Amine 2002 Layered  $\text{Li}(\text{Ni}_{0.5-x}\text{Mn}_{0.5-x}\text{M}_{2x})\text{O}_2$  ( $\text{M}'=\text{Co, Al, Ti}$ ;  $x=0, 0.25$ ) cathode materials for Li-ion rechargeable batteries *Power Sources* **112** pp 41-48.
- [11] Liu J, Wang Q, Reeja Jayan B and Manthiram A 2010 Carbon-coated high capacity layered  $\text{Li}[\text{Li}_{0.54}/0.13/0.132]$  cathodes *Electrochemistry Communications* **12**(6) pp 750-753.
- [12] Kang S, H Kempgens, Greenbaum Kropf and A J 2007 Interpreting the structural and electrochemical complexity of  $0.5\text{Li}_2\text{MnO}_3 \cdot 0.5\text{LiMO}_2$  electrodes for lithium batteries ( $\text{M} = \text{Mn}_{0.5-x}\text{Ni}_{0.5-x}\text{Co}_{2x}$ ,  $0 \leq x \leq 0.5$ ). *J.mater.chem.*, **17**, pp 2060-2077.
- [13] Z Lu and J R Dahn 2002 Understanding the anomalous capacity of  $\text{Li/Li}[\text{Ni}_x\text{Li}_{(1/3-2x/3)}\text{Mn}_{(2/3-x/3)}]\text{O}_2$  cells using in situ x-ray diffraction and electrochemical studies *Electrochem. Soc* **149** pp A815-A822.
- [14] Chenhao Zhao, Xinxin Wang, Xinru Liu, et al 2014 Mn-Ni Content-Dependent Structures and Electrochemical Behaviors of Serial  $\text{Li}_{1.2}\text{Ni}_{0.13+x}\text{Co}_{0.13}\text{Mn}_{0.54-x}\text{O}_2$  as Lithium-Ion Battery Cathodes *American Chemical Society* **6** pp 2386-2392.
- [15] S H Park, S H Kang, C S Johnson, K Amine 2009 *J. Mater, Chem.* **19** pp 4510-4516
- [16] Kitaura H, Hayashi A, Tadanaga K, Tatsumisago M 2010 Electrochemical performance of all-solid-state lithium secondary batteries with Li-Ni-Co-Mn oxide positive electrode *Electrochim Acta* **55** pp 8821-8828.
- [17] Kim J M and Chung H T 2004 Effect of lithium boron oxide glass coating on the electrochemical performance of  $\text{LiNi}_{1/3}\text{Co}_{1/3}\text{Mn}_{1/3}\text{O}_2$  *Electrochim Acta* **49** pp 937-944.
- [18] Y J Hong, S H Choi, C M Sim, J K Lee and Y C Kang 2012 Effect of boric acid on the properties of  $\text{Li}_2\text{MnO}_3 \cdot \text{LiNi}_{0.5}\text{Mn}_{0.5}\text{O}_2$  composite cathode powders prepared by large-scale spray pyrolysis with droplet classifier *MRS Bull* **47** pp 4359-4364.
- [19] C H Zhao, W P Kang, Q B Xue and Q Shen 2012 Polymerization pyrolysis-assisted nanofabrication of solid solution  $\text{Li}_{1.2}\text{Ni}_{0.13}\text{Co}_{0.13}\text{Mn}_{0.54}\text{O}_2$  for lithium-ion battery cathodes *Nanopart.Res.* **14**(1240) pp1-9.